High-resolution record of the Matuyama–Brunhes transition constrains the age of Javanese *Homo erectus* in the Sangiran dome, Indonesia

Masayuki Hyodo[a,b,1], Shuji Matsu'ura[c], Yuko Kamishima[b], Megumi Kondo[c], Yoshihiro Takeshita[d], Ikuko Kitaba[a], Tohru Danhara[e], Fachroel Aziz[f], Iwan Kurniawan[f], and Hisao Kumai[g]

[a]Research Center for Inland Seas, and [b]Department of Earth and Planetary Sciences, Kobe University, Kobe 657-8501, Japan; [c]Laboratory of Physical Anthropology, Ochanomizu University, Tokyo 112-8610, Japan; [d]Faculty of Education, Shinshu University, Nagano 380-8544, Japan; [e]Kyoto Fission-Track Corporation, Kyoto 603-8832, Japan; [f]Centre for Geological Survey, Geological Agency, Bandung 40122, Indonesia; and [g]Department of Geoscience, Osaka City University, Osaka 558-8585, Japan

Edited by Tim D. White, University of California, Berkeley, CA, and approved October 21, 2011 (received for review August 10, 2011)

A detailed paleomagnetic study conducted in the Sangiran area, Java, has provided a reliable age constraint on hominid fossil-bearing formations. A reverse-to-normal polarity transition marks a 7-m thick section across the Upper Tuff in the Bapang Formation. The transition has three short reversal episodes and is overlain by a thick normal polarity magnetozone that was fission-track dated to the Brunhes chron. This pattern closely resembles another high-resolution Matuyama–Brunhes (MB) transition record in an Osaka Bay marine core. In the Sangiran sediments, four successive transitional polarity fields lie just below the presumed main MB boundary. Their virtual geomagnetic poles cluster in the western South Pacific, partly overlapping the transitional virtual geomagnetic poles from Hawaiian and Canary Islands' lavas, which have a mean $^{40}Ar/^{39}Ar$ age of 776 ± 2 ka. Thus, the polarity transition is unambiguously the MB boundary. A revised correlation of tuff layers in the Bapang Formation reveals that the hominid last occurrence and the tektite level in the Sangiran area are nearly coincident, just below the Upper Middle Tuff, which underlies the MB transition. The stratigraphic relationship of the tektite level to the MB transition in the Sangiran area is consistent with deep-sea core data that show that the meteorite impact preceded the MB reversal by about 12 ka. The MB boundary currently defines the uppermost horizon yielding *Homo erectus* fossils in the Sangiran area.

paleomagnetism | marine isotope stage 19 | magnetostratigraphy | geochronology

From its origins in Africa, or perhaps the southern Caucasus (1, 2), *Homo erectus* (*sensu lato*) dispersed across Asia, arriving in Java sometime in the Calabrian Age of the Early Pleistocene [*ca.* 1.8 Ma to *ca.* 0.8 Ma, the second stage/age of the recently revised (3) Pleistocene] (e.g., 4–6). Among the *H. erectus* sites outside Africa, fossil localities in Java provide a long history of collection and study in multiple locations compared with others in western Asia (7, 8) and China (9–11). In the 1891–1892 excavation at Trinil, East Java, E. Dubois discovered a hominid skull cap and femur, which triggered numerous follow-up collections in Java. To date, fossils attributed to *H. erectus* have been found in Sangiran, Sambungmacan, Trinil, Ngandong, Ngawi, Kedungbrubus, and Perning (Mojokerto), all located in a narrow zone extending about 200 km east–west in Central to East Java (Fig. S1). These fossil sites have been associated with a wide range of ages. Although some chronometric dates are controversial, *H. erectus* seems to have been present in Java for a long duration, ranging from the Early Pleistocene into the Late Pleistocene. Therefore, Javanese hominids provide an important resource for human evolutionary studies outside Africa.

The Sangiran dome area, Central Java, has yielded a number of hominid fossils since 1936. The thick (>300-m) sedimentary sequence is one of the standard Plio-Pleistocene sections in Java. However, it lacks an accepted chronostratigraphy. The $^{40}Ar/^{39}Ar$ date of 1.66 Ma reported for two specimens described as the oldest hominid remains in the Sangiran area (12) is ∼0.5 million y older than previous age estimates for that site (13–15). This date has been questioned because of the uncertain stratigraphic relationship between the dated pumice and the hominid fossils (9, 16–18). Subsequently reported $^{40}Ar/^{39}Ar$ dates for the Sangiran hominids (18) modify this chronology, but are still inconsistent with the magnetic polarity stratigraphy (9) and other $^{40}Ar/^{39}Ar$ dates (19). Thus, the controversy over the "long" (older) and "short" (younger) chronologies for the hominid-bearing sediments is still ongoing (e.g., 20).

The goal of this study is to produce a reliably dated stratigraphic level (age datum) in the Sangiran dome. Here we focus on the upper portion of the hominid fossil-bearing horizons, whereas previous studies mostly concentrated on the lower end. Our work examines the dome's topmost formation, which has not yet yielded hominid fossils and has never been investigated in detail.

Geologically, the Sangiran area is a dome structure, extending 8 km north–south and 4 km east–west, located southwest of the Kendeng Hills (Fig. S1). The dome was truncated by erosion, exposing a concentric pattern of strata, with older strata surrounded by younger (Fig. 1*A*) (21). The exposed Plio-Pleistocene sediments are divided into four units (13). The marine Puren (Kalibeng) Formation lies at the base (Fig. 1*B*), overlain by the Sangiran (Pucangan) Formation, consisting of shallow marine to lagoonal sediments below lacustrine sediments. The Sangiran Formation is overlain by the Bapang (Kabuh) Formation, and further by the Pohjajar (Notopuro) Formation (Fig. 1). The upper two formations are primarily fluviatile sediments intercalated with many layers of pumice, volcanic ash, and lahar. There are three active volcanoes within 50 km of Sangiran: Mt. Lawu to the southeast, and Mts. Merapi and Merbabu to the west (Fig. S1). These volcanoes are candidates for the source of volcanic materials in the Sangiran dome.

Hominid-bearing horizons in the dome range from the Upper Tuff (UT) of the Bapang Formation down to Tuff 11 in the Sangiran Formation (13) (Fig. 1*B*) or possibly slightly lower (22). The southeast sector of the dome has yielded many hominid fossils, including ∼10 well-preserved cranial and mandibular specimens (Fig. 1*A*). The type sections of the Bapang and

Author contributions: M.H. and S.M. designed research; M.H., S.M., Y.K., M.K., Y.T., I. Kitaba, T.D., F.A., I. Kurniawan, and H.K. performed research; M.H., Y.K., I. Kitaba, and T.D. analyzed data; and M.H. and S.M. wrote the paper.

The authors declare no conflict of interest.

This article is a PNAS Direct Submission.

Freely available online through the PNAS open access option.

[1]To whom correspondence should be addressed. E-mail: mhyodo@kobe-u.ac.jp.

This article contains supporting information online at www.pnas.org/lookup/suppl/doi:10.1073/pnas.1113106108/-/DCSupplemental.

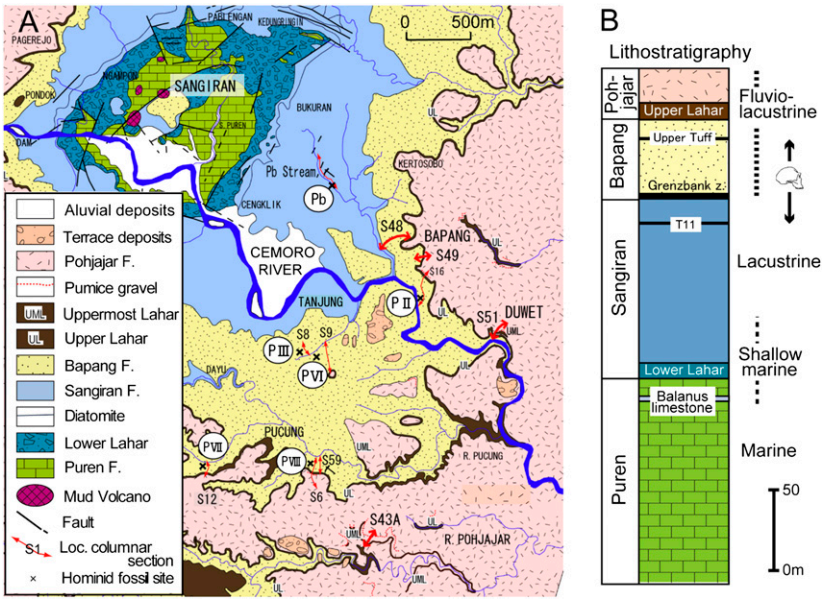

Fig. 1. Geological map (*A*) and lithostratigraphy (*B*) of the Sangiran area. In *A*, thick red arrows show the sections (S48, S49, D51, and S53A) sampled for paleomagnetic analysis. Crosses show *H. erectus* fossil sites: mandible *Pithecanthropus* b (Pb), calotte *Pithecanthropus* II (P II), calotte *Pithecanthropus* III (P III), calotte *Pithecanthropus* VI (P VI), calotte *Pithecanthropus* VII (P VII), and cranium *Pithecanthropus* VIII (P VIII).

Pohjajar Formations, the targets of our study, are also located in this sector (21): at S48 (geological columnar section site 48) and S49 near Bapang village, and at S43 (S43A, B, C) upstream of the Pohjajar River, respectively (Fig. 1*A*).

We first conducted a geological survey, searching for sections that included fine sediments. For the Pohjajar Formation, we selected the section at S51 near Duwet village in addition to the main type section at S43A (Fig. 1*A*). For the Bapang Formation, we selected the type sections at S48 and S49. Paleomagnetic sampling tracts are indicated by the red arrows in Fig. 1*A*. Most of the Bapang samples are from channel deposits of silts or tuffaceous silts, except for a high-resolution sequence, 11 m thick, across the UT layer at S48 and S49. This sequence primarily consists of clays, clayey silts, and silts that were deposited in still waters. Parallel sample series were collected from S48 and S49 (Fig. 1*A* and Fig. S2). A total of 436 specimens was collected from 92 horizons.

UT is pinkish, about 50 cm thick at S48 and 60 cm thick at S49. During fieldwork, we recognized three more pinkish tuff layers above UT. We designate them Upper Tuff 0.5 (UT0.5), Upper Tuff 1 (UT1), and Upper Tuff 2 (UT2) in ascending order. UT0.5 and UT1 are found at both sites, whereas UT2 is seen only at S49. UT1 is 15–40 cm thick, and was described previously as an unnamed tuff by Itihara et al. (21). Tuffs UT0.5 and UT2, 1–10 cm thick, have not been described yet. These tuffs were used for precise stratigraphic correlations between S48 and S49. Samples were collected at 10- to 30-cm intervals for the high-resolution sequence across UT (Fig. S2). UT correlatives near Pucung (at S59) and Tanjung (at S9) on the opposite side of the Cemoro River (Fig. 1*A*) were also sampled.

For tuff analyses, we collected samples of UT and UT1 at S48, UT, UT0.5, UT1, and UT2 at S49, and UT at S59 and S9. We also sampled the Upper Middle Tuff (UMT) at S48, which is another pinkish tuff about 6 m below UT at the type site of the Bapang Formation (Fig. 1*A*).

Results

Progressive thermal demagnetizations (THDs) in steps above 250–300 °C or alternating field demagnetizations (AFDs) in steps above 10–30 millitesla (mT) were used to isolate a primary remanent magnetization (Fig. S3 *A* and *B*). The two methods provide the same results. THDs could not be applied to samples collected using titanium tubes or samples of fragile silts or fine sands. About 25% of specimens were subjected to THD, covering about 60% of horizons.

THD results show unblocking temperatures at 500–580 °C and 680 °C, suggesting dominant carriers are magnetite (titanomagnetite) and hematite, respectively (Fig. S3*J*). The same carriers were suggested by the thermomagnetic analysis results from samples possessing transitional polarity and short reversal fields (Fig. S3 *K* and *L*).

For most samples, characteristic remanent magnetizations (ChRMs) were calculated by principal component analysis. When the stepwise THD or AFD result did not show a remanence vectorial decay to the origin and the remanence direction at each step moved on a great circle (GC) (Fig. S3 *G* and *H*), we determined a GC for each specimen. This allowed us to calculate a mean horizon direction (23). For some horizons, a mean direction was calculated using ChRMs and GCs. The mean directions were bedding plane-corrected, and generally tilt was 5–10°. The horizons based on GC calculations are all below UT1 in the Bapang Formation. We discarded data on 20 horizons where the number of specimens that provided either ChRM or GC was less than three.

A mean direction whose virtual geomagnetic pole (VGP) latitude is in the northern/southern hemisphere is defined as normal/reverse polarity. Above UT1 all horizons show normal polarity, whereas the horizons at and below UMT have reverse polarity (Fig. S2 and Table S1). Transitional polarity fields, defined as those with VGP latitudes lower than 45°, lie just above UT0.5 (Fig. S2). The combined plot of paleomagnetic results for S48 and S49 over an 11-m–thick section across UT reveals multiple short reversal episodes (Fig. S4*F*).

It is noteworthy that the "UT correlatives" at Pucung (S59) and Tanjung (S9) show reverse polarity (Table S1, nos. 91 and 92). The Pucung and Tanjung UT correlatives are paleomagnetically different from the normal polarity Bapang UT (S48, S49; Fig. S2).

As mentioned above, horizons where the GC method was applied are all below UT1, and also are in the zone of low

normalized natural remanent magnetization (NRM) intensity (Fig. S4*H*). The stratigraphic levels of horizons providing no reliable mean direction (Fig. S4*A*) also lie in the low normalized NRM intensity or near short reversals (Fig. S4 *F* and *H*). From these observations, we suggest that the difficulty in identification of a reliable paleomagnetic direction is due to the low efficiency in aligning magnetic grains in weak fields or during directional fluctuations.

The difference in magnetic polarity among the UT correlatives suggests that these tuffs are not correctly correlated. Hornblende refractive indices in the pinkish tuff layers in the Bapang Formation (Fig. S5 and Table S2) are bimodal. One group of tuffs, UT2, UT1, UT0.5, and UT from the Bapang sites (S48 and S49), has a primary mode at ∼1.679–1.681. The other group, UMT at Bapang (S48), and the UT correlatives at Pucung (S59) and Tanjung (S9) have a dominant mode at 1.689–1.690. This result suggests that the Pucung and Tanjung UT correlatives (21) are not correlative with the Bapang UT in the type sections (Fig. 1*A*), rather that these UT correlatives, south of the Cemoro River, are correlative with UMT at Bapang. This correlation is supported by the mineral compositions (Table S2) and magnetic polarity (Fig. S2).

Discussion

Magnetic Polarity Stratigraphy. The present paleomagnetic result defines three magnetic polarity zones. A thick (*ca.* 30-m) reverse polarity zone continues from the base to below the UT in the Bapang Formation (Fig. S2). This zone is overlain by a 7-m–thick mixed polarity zone that ranges in level from about 3.5 m below UT up to just below UT1 (Fig. S2), above which a thick (*ca.* 50-m) normal polarity zone continues to the upper part of the Pohjajar Formation.

In the upper Pohjajar Formation, a revised zircon fission-track age of 0.18 ± 0.02 Ma (24) has been obtained for the Upper Pumice Tuff that was previously fission track-dated to 0.25 ± 0.07 (here, 2σ) Ma (25). The previous age was not calibrated to standard samples of known age, and the disagreement with the revised age may be due to lack of calibration. Other age estimates of the Pohjajar Formation came from hornblende extracts and an andesite rock sample, yielding $^{40}Ar/^{39}Ar$ ages of 0.50 Ma [error not stated (26)] for the middle part of the formation and of 0.15 ± 0.01 Ma [detailed stratigraphic level not identified (27)], respectively. Even with these uncertainties, the thick normal polarity zone should be correlated with the Brunhes chron. Thus, the reverse polarity zone is reasonably correlated with the Matuyama chron, and the mixed polarity zone with the Matuyama-to-Brunhes (MB) polarity transition.

Polarity Transition Features. Using the base of UT as a datum, we define the main MB boundary (MBB) at 170 cm in elevation (Fig. S4*F*, arrow), above/below which normal/reverse polarity fields are dominant. We further define three short reversal episodes that lie at −350 cm, at an elevation range of 0–70 cm including UT, and just below UT1, here designated E1, E2, and E3, respectively (Fig. S4*F*). The ChRM directions are well-determined for these episodes (Fig. S3 *D*–*F*). The MB polarity transition ranging from E1 to just above E3 coincides with the low normalized NRM intensity zone (Fig. S4*H*).

MB polarity transition records from high-average accumulation rate (a.r.) sediments (>50 cm/ka) have short reversal episodes similar to those observed here. In an Osaka Bay marine core, a 6-m long MB transition record lies within the low relative paleointensity zone (28). The transition has a short episode named "a" that is 4.56 m to 4.0 m below the main MBB, and short episodes, about 20 cm thick, named "b" and "c" lie at 1.1 m below and 0.4 m above the boundary (Fig. 2*B*). In the high-a.r. marine silt sequence in the Boso Peninsula, eastern Japan (32), thick and thin short reversal episodes lie at 6.2–5.3 m and 1.9 m below the main MBB, respectively. Thus, the timings of these short reversal episodes are very similar. A plausible correlation of the E1 and E3 in Sangiran with the "a" and "c" in Osaka Bay (Fig. 2 *A* and *B*) provides an average a.r. estimate of *ca.* 70 cm/ka for the Bapang Formation type sections.

MB polarity transition records from low-a.r. (about 10 cm/ka or less) sediments such as deep-sea cores or Chinese loess sediments show somewhat different features. They have multiple polarity swings within depth intervals of 40–60 cm (33–35), but the numbers of changes are different. This difference can be

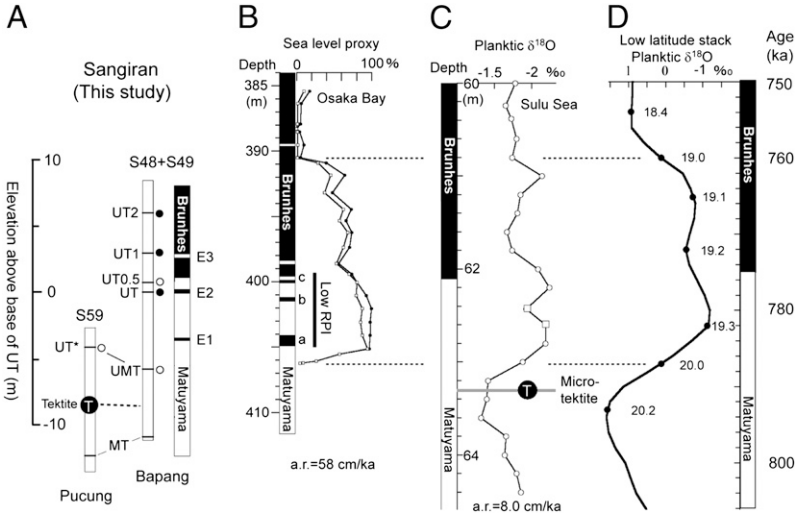

Fig. 2. Correlation of the magnetic polarity stratigraphy records across the MB transition. (*A*) The magnetic polarity stratigraphy from the Sangiran area. UT* in the columnar section at S59 was previously correlated with UT at the Bapang-type sections (S48+S49), but is now correlative with UMT at S48 (see text). Solid/open circles show normal/reverse magnetic polarity. (*B*) The magnetic polarity and diatom-based sea-level proxy from the Osaka Bay 1,700-m core (28). The bar shows the low relative paleointensity (RPI) zone. The sea-level proxy curve with solid circles represents the values of 100 minus the percentage of freshwater diatoms, and that with open circles represents the percentages of marine and brackish water diatoms. (*C*) The magnetic polarity and planktic $\delta^{18}O$ from the Sulu Sea (ODP site 769) after Schneider et al. (29). The magnetic polarity boundary is shifted upward by 15 cm because of the effect of delayed lock-in (30). (*D*) Low-latitude stack of planktic $\delta^{18}O$ and magnetic polarity stratigraphy after Bassinot et al. (31).

caused by both the different resolution available at smaller a.r. and the filtering effect due to the magnetization process (36). Jin and Liu (37) have recently shown that although the Chinese loess-paleosol sediments can record a transition, the detailed field morphology is poorly defined due to the low alignment efficiency of magnetic grains in a weak field undergoing transition.

The Sangiran MB transition has four successive transitional polarity fields with VGP latitudes lower than 45° recorded in a 30-cm–thick section just below the main MBB (Fig. S4*E*). The VGPs cluster in the western South Pacific (Fig. S6), partly overlapping the VGP cluster from the transitionally magnetized lavas of the Hawaii and Canary Islands (38). The combined average $^{40}Ar/^{39}Ar$ age of these lavas is 776 ± 2 ka. The agreement of the VGP clusters suggests the transitional fields have a dipolar nature. From the average a.r. estimated above, the thickness of 30 cm provides an estimate of about 400 y for the transitional polarity field zone. Our 10-cm^3 specimen of 2.2-cm thickness would correspond to about 30 y, and thus can easily resolve this short (*ca.* 400-y) event. The Sangiran transitional VGPs are clearly separated from the VGP cluster for the precursor event that is centered in north to southwestern Australia and $^{40}Ar/^{39}Ar$-dated at 793–795 ka (38).

The agreement of the VGP clusters (Fig. S6) demonstrates that the 30-cm–thick transitional field zone is very likely 776 ka (38) in age. This zone is about 2 m below (3 ka before, based on average a.r.) the termination of the MB transition, and about 5 m above (7 ka after) its onset (Fig. S4). Thus, the Sangiran MB transition spans 783–773 ka, consistent with the Osaka Bay core data (785–775 ka) (28). We can see a similar duration (783–770 ka) for a multiple polarity swing zone with low paleointensity in a North Atlantic deep-sea core record from Ocean Drilling Program (ODP) site 984 (39). However, other North Atlantic cores seem to have shorter and younger transition zones (775–771 ka) (39). The difference may be an artifact of the low a.r. of deep-sea sediments. Precise dating of the MB boundary has proven difficult due to the complexity and duration of the multiple-reversal transition zone. Our study shows the relationship of the VGP at 776 ka to the MB transition zone, but clearly more studies of high-a.r. sediments are needed.

UT Correlatives at Pucung and Tanjung. As mentioned above, the heavy mineral compositions and hornblende refractive indices show that the Pucung and Tanjung UT layers are clearly distinct from UT of the type sections at Bapang (S48 and S49); rather, they should be correlated with Bapang UMT (Fig. 2*A*). The paleomagnetic data support this correlation. Bapang UT has normal polarity. Pucung and Tanjung UT correlatives and Bapang UMT all have reverse polarity (Fig. S2 and Table S1). Thus, we propose that the pinkish tuff layers at Pucung and Tanjung previously correlated with UT (21) are actually correlated with UMT in the Bapang S48 type section. The UT layer is the thickest among the four pinkish tuff layers at Bapang, and the sections at Pucung and Tanjung intercalate only one pinkish tuff layer. These circumstances may have led to the earlier miscorrelation.

Tektite Horizon Underlying the MB Transition. Tektites are natural glass objects produced by the melting of crustal material during large-impact cratering events (40, 41). The Australasian tektite field extends from southern China to the Southern Ocean and from the Western Pacific to southwestern Indian Ocean (42). The Sangiran area yields a number of tektites, but only two pieces were found in situ during excavations. The Indonesia–Japan joint research CTA-41 Project, 1977–1979 (13), found a tektite about 4 m above the Middle Tuff (MT) of the Bapang Formation at Brangkal (Fig. 3, S39) (43). Another tektite was found at almost the same stratigraphic level, 3.6 m above the MT at Pucung (Fig. 3, S59), about 6 km south of Brangkal (43, 44). An estimated tektite correlative level at S48 (Fig. 2*A*) is 10.6 m below (15 ka before, based on average a.r.) the main MBB and 5.4 m below (8 ka before) E1. Thus, the tektite horizon clearly pre-dates the MB transition. Comparison with the Osaka Bay data (Fig. 2 *A* and *B*) suggests the tektite horizon is correlated with marine oxygen isotope stage (MIS) 20. This result is consistent with the Sulu and Celebes Seas cores' data that a microtektite layer lies *ca.* 12 ka before the MB boundary in MIS 20 (29) (Fig. 2 *A* and *C*).

Hyodo et al. (15) reported a normal magnetic polarity just above the tektite level at Pucung (S59), and interpreted it as the earliest Brunhes. This normal polarity level is now clearly just below the UMT, and can be correlated with the precursor event in MIS 20 (45).

The stratigraphic position of tektites in the Sangiran area was called into question, suspected of being reworked from younger deposits (18, 20), because no additional in situ tektites have been recovered and because of inconsistencies in the $^{40}Ar/^{39}Ar$-dating results (see below). The present study, however, clearly supports the presence of in situ tektites between MT and UT as revealed by the CTA-41 Project (13).

Comparison with Previous Paleomagnetic and $^{40}Ar/^{39}Ar$-Dating Results. Previous paleomagnetic studies (14, 15, 46) are not as detailed as this study at the MB transition. Hyodo et al. (15) determined MBB just below UT, based on data obtained south of the Cemoro River. Those data should be reexamined in combination with tuff analyses because of the correlation problems across the river for the pinkish tuffs (UT vs. UMT). The complex polarity changes in the lower Bapang Formation reported by Shimizu et al. (46) are likely due to insufficient removal of secondary viscous remanent magnetization, because their AFD level was below 20–30 mT.

Hornblende samples from pumice collected from the lowermost part of the Bapang Formation are $^{40}Ar/^{39}Ar$-dated at 0.86 ± 0.03 Ma and 0.88 ± 0.01 Ma (19). These dates are consistent with the present magnetic polarity stratigraphy. Larick et al. (18) reported hornblende $^{40}Ar/^{39}Ar$ dates that are significantly older than these results. For example, the Bapang UT layer, which we argue lies within the MB transition, was dated at 1.02 ± 0.06 Ma, and pumice layers close to the MT level were dated at 0.98 ± 0.11 Ma, 1.02 ± 0.13 Ma, 1.24 ± 0.12 Ma, and 1.27 ± 0.18 Ma. The older $^{40}Ar/^{39}Ar$ dates may be related to reworking of epiclastic pumice balls in the Bapang Formation from older deposits.

Finally, Australasian tektites from the Bose Basin of southern China were $^{40}Ar/^{39}Ar$-dated to 803 ± 3 ka (47). This age can be associated with the tektite level between MT and UMT and is consistent with the present magnetic polarity stratigraphy.

Horizon of Hominid Occurrence in the Sangiran Area. The Sangiran *H. erectus* materials, variously referred to as *Pithecanthropus* and *Meganthropus*, constitute the majority of existing Early Pleistocene hominid fossils from Java. Although most of the Sangiran specimens were found by chance by local inhabitants, sometimes retrieved without precise provenance, geological and geochemical investigations have shown that the hominid fossils derive from sediments between the UT of the Bapang Formation and Tuff 11 (13) or possibly a slightly lower level (22) of the Sangiran Formation. In light of paleontologic and stratigraphic contexts, the Sangiran *H. erectus* remains are tentatively divided into chronologically older and younger groups (48–50).

The chronologically older group is derived from the uppermost Sangiran Formation and the Grenzbank zone, the basal layer of the Bapang Formation. It is associated with the Ci Saat fauna or the Trinil H.K. fauna; this group includes mandibles *Pithecanthropus* B (Sangiran 1b) and F (Sangiran 22), calotte *Pithecanthropus* II (Sangiran 2), cranium *Pithecanthropus* IV (Sangiran 4), and mandibles *Meganthropus* A (Sangiran 6a) and B (Sangiran 8). *Pithecanthropus* II was previously placed at just

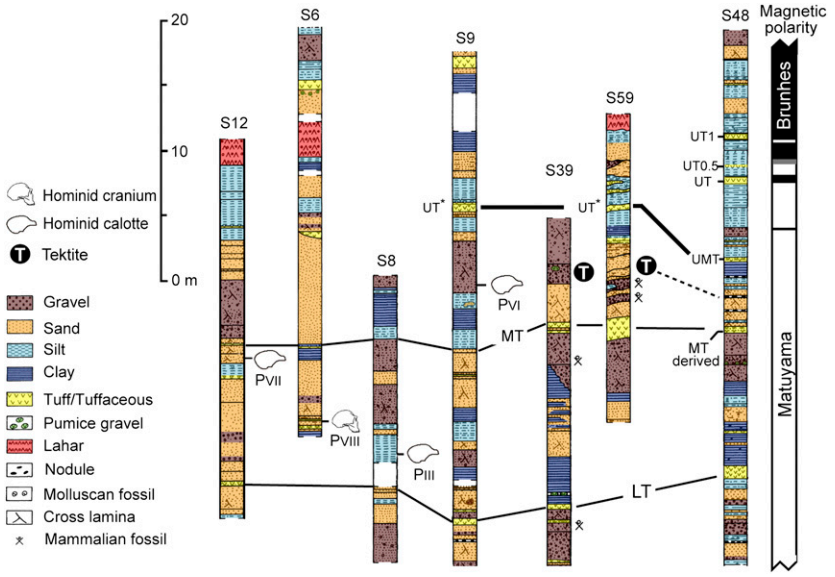

Fig. 3. Lithostratigraphy of the Bapang Formation sections, showing the stratigraphic level of the two in situ tektites and some of the *H. erectus* cranial remains. The transitional zone in the magnetic polarity stratigraphy is shown in gray. UT* in the columnar sections (S9, S59) was previously correlated with UT (21) but is now correlative with UMT (see text).

below MT (21), but should be relocated to the Grenzbank zone based on bone fluorine content (22) and a geological resurvey of the find site (51).

The chronologically younger group is derived from sediments near the MT in the Bapang Formation (Fig. 3), and is associated with the Kedung Brubus fauna; this group includes calottes *Pithecanthropus* III (Sangiran 3), VI [Sangiran 10, also referred to as the sixth skull cap or *Pithecanthropus* V (52)], and VII (Sangiran 12), cranium *Pithecanthropus* VIII (Sangiran 17), cranium skull IX (Tjg-1993.05), and mandibles Sb 8103 and Ng 8503 (48). In Fig. 3, the horizon that was reported to have yielded the *Pithecanthropus* VI calotte discovered at the Tanjung S9 site is placed just below the midpoint between MT and the UT correlative. Multielement analyses of the specimen (53) have verified its derivation from between MT and the UT correlative (now correlated with UMT). With this placement, the stratigraphic provenance of *Pithecanthropus* VI provides a solid uppermost datum of the hominid fossils in the Sangiran area. This stratigraphic level is nearly the same as the tektite horizon at the Brankal S39 site.

The approximate coincidence of the hominid last occurrence and the tektite level in this area could imply a tektite fall effect on Sangiran hominids or a possible reduction of the Javanese *H. erectus* population, although cranial morphology suggests a long-term continuous, gradual evolution of Javanese *H. erectus* (49) from the Sangiran hominids around the MT (Early Pleistocene) to the Ngandong hominids (Late Pleistocene) via the Sambungmacan hominids (probably Middle Pleistocene) (Fig. S1). Vertebrate paleontology also suggests continuity between the Kedung Brubus fauna of the Sangiran area and the Middle Pleistocene fauna from Sambungmacan (54).

Very recently, Zaim et al. (55) have reported, based on the long (older) chronology, a new "1.5 million-year-old *Homo erectus* maxilla" from the basal layer of the Bapang Formation. Our data, showing the near co-occurrence of the tektite level and the magnetostratigraphic constraint, argue that the Sangiran hominid last occurrence is dated to *ca.* 0.79 Ma. In addition, the short (younger) chronology is strongly supported by $^{40}Ar/^{39}Ar$ dates of 0.86–0.88 Ma (17) in the lower Bapang Formation and the absence of the Jaramillo subchronozone (Fig. S2). Therefore, the 1.5 million-year-old age needs to be reevaluated.

Conclusion

Paleomagnetic analyses conducted on the Bapang and Pohjajar Formations in the Sangiran area, Java, reveal a 7-m–thick MB transition zone that just overlies the UMT. Features of the transition, with three short reversal episodes, are well-correlated with other MB transition records from high-a.r. (>50 cm/ka) sediments from Osaka Bay and Boso Peninsula, Japan. Four transitional polarity fields that occur in a 30-cm section just below the main MB boundary show a VGP cluster partly overlapping that from the transitionally magnetized lavas from the Hawaii and Canary Islands dated at 776 ± 2 ka. The mineral composition, refractive index, and magnetic polarity of tuffs reveal that the pinkish tuff layer at Pucung and Tanjung, previously correlated with UT, is actually correlated with UMT at the Bapang S48 type section. Both the latest occurrence of hominid fossils and the tektite source bed in the Sangiran area lie just below the UMT level. The MB transition starts about 2 m above UMT. Therefore, the MB transition constrains the uppermost age of Sangiran *H. erectus* to about 0.79 Ma.

Methods

Paleomagnetic Sampling and Analysis. We primarily collected oriented block samples, from which cubic specimens within 5 cm in depth were cut and put into cubic capsules 10 cm^3 in volume. From soft sediments, specimens were collected and put into capsules in the field, using a tool (9). All specimens were subjected to progressive THD or AFD in 10–15 steps. For magnetic analyses, we used a 2G cryogenic magnetometer, a Bartington MS2 susceptibility meter, and a Curie balance.

Tuff Analyses. A subsample of each tuff sample was washed on a 63-μm sieve and examined under a binocular microscope. No glass was found in the samples. The remnant of each sample was then washed on 63-, 125-, and 250-μm mesh sieves. The 63- to 125-μm fraction was mounted on glass slides, and the bulk grain composition and heavy-mineral composition were determined under a microscope. Refractive indices of hornblende crystals were measured individually using a refractive index measurement system (RIMS) analyzer (56). In the absence of volcanic glass, hornblende refractive indices (controlled by the content of oxides with high specific refractivity) were used to distinguish tuffs, as in the cataloged data for tuffs in Japan (57).

ACKNOWLEDGMENTS. We thank Erick Setiyabudi, Mr. Suyono, and the late Mr. Sudijono for collaboration; David L. Dettman for correcting the English of the manuscript and giving helpful suggestions; and two

anonymous reviewers for giving useful comments. I. Kitaba is a Japan Society for the Promotion of Science Research Fellow. This study is supported by funds from the Japan Society for the Promotion of Science (Grants 13440255, 1540315, 18200053, and 22320154) and partly performed under the cooperative research program of Center for Advance Marine Core Research, Kochi University (CMCR) (05B020, 09A006). This work was carried out under the auspices of the Center for Geological Survey, Geological Agency, Indonesia.

1. Ferring R, et al. (2011) Earliest human occupations at Dmanisi (Georgian Caucasus) dated to 1.85–1.78 Ma. *Proc Natl Acad Sci USA* 108:10432–10436.
2. Wood B (2011) Did early *Homo* migrate "out of" or "in to" Africa? *Proc Natl Acad Sci USA* 108:10375–10376.
3. Gibbard PL, et al. (2010) Formal ratification of the Quaternary System/Period and the Pleistocene Series/Epoch with a base at 2.58 Ma. *J Quat Sci* 25:96–102.
4. Dennell R, Roebroeks W (2005) An Asian perspective on early human dispersal from Africa. *Nature* 438:1099–1104.
5. Ciochon RL, Bettis, EA, III (2009) Palaeoanthropology: Asian *Homo erectus* converges in time. *Nature* 458(7235):153–154.
6. Matsu'ura S (2010) Jinrui saishono shutu-Afurika (out of Africa) to touhou-Ajia heno kakusan mondai [Initial hominid dispersal 'Out of Africa' and a reconsideration of the general model of rapid migration to eastern Asia prior to 1.5 Ma.]. *Quaternary Research (Japan)* 49:293–298 (in Japanese with English abstract).
7. Gabunia L, Vekua AA (1995) A Plio-Pleistocene hominid from Dmanisi, East Georgia, Caucasus. *Nature* 373:509–512.
8. Belmaker M, Tchernov E, Condemi S, Bar-Yosef O (2002) New evidence for hominid presence in the Lower Pleistocene of the Southern Levant. *J Hum Evol* 43(1):43–56.
9. Hyodo M, et al. (2002) Paleomagnetic dates of hominid remains from Yuanmou, China, and other Asian sites. *J Hum Evol* 43(1):27–41.
10. Zhu RX, et al. (2004) New evidence on the earliest human presence at high northern latitudes in northeast Asia. *Nature* 431:559–562.
11. Zhu RX, et al. (2008) Early evidence of the genus *Homo* in East Asia. *J Hum Evol* 55: 1075–1085.
12. Swisher, CC, III, et al. (1994) Age of the earliest known hominids in Java, Indonesia. *Science* 263:1118–1121.
13. Watanabe D, Kadar N, eds (1985) *Quaternary Geology of the Hominid Fossil Bearing Formations in Java* (Geological Research and Development Centre, Bandung, Indonesia).
14. Hyodo M, Sunata W, Susanto EE (1992) A long-term geomagnetic excursion from Plio-Pleistocene sediments in Java. *J Geophys Res* 97:9323–9335.
15. Hyodo M, Watanabe N, Sunata W, Susanto EE, Wahyono H (1993) Magnetostratigraphy of hominid fossil bearing formations in Sangiran and Mojokerto, Java. *Anthropol Sci* 101:157–186.
16. de Vos J, Sondaar PY (1994) Dating hominid sites in Indonesia. *Science* 266:1726–1727.
17. Sémah F, Saleki H, Falguères C, Féraud G, Djubiantono T (2000) Did Early Man reach Java during the Late Pliocene? *J Archaeol Sci* 27:763–769.
18. Larick R, et al. (2001) Early Pleistocene $^{40}Ar/^{39}Ar$ ages for Bapang Formation hominins, Central Jawa, Indonesia. *Proc Natl Acad Sci USA* 98:4866–4871.
19. Saleki H, et al. (1998) Radiometric dating of *Homo erectus* bearing Kabuh layers at Ngebung (Sangiran, Central Java, Indonesia). *Actes du XIIIe Congrès UISPP Forli Italie* 2:63–74 (in French).
20. Bettis, EA, III, et al. (2009) Way out of Africa: Early Pleistocene paleoenvironments inhabited by *Homo erectus* in Sangiran, Java. *J Hum Evol* 56(1):11–24.
21. Itihara M, et al. (1985) Geology and stratigraphy of the Sangiran area. *Quaternary Geology of the Hominid Fossil Bearing Formations in Java*, eds Watanabe N, Kadar D (Geological Research and Development Centre, Bandung, Indonesia), pp 11–43.
22. Matsu'ura S (1982) A chronological framing for the Sangiran hominids: Fundamental study by the fluorine dating method. *Bull Natl Sci Mus Tokyo Ser D* 8:1–53.
23. McFadden PL, McElhinny MW (1988) The combined analysis of remagnetization circles and direct observations in paleomagnetism. *Earth Planet Sci Lett* 87:161–172.
24. Danhara T, et al. (2007) Towards the reconstruction of the fission-track chronology of Javanese palaeoanthropological sites based on volcanic ash analysis and the evaluation of the dating samples. *International Symposium on Quaternary Environmental Changes and Humans in Asia and the Western Pacific. Geol Sur Japan Inter Report.* No 42 (Geological Survey of Japan, Tsukuba, Japan), pp 58–59.
25. Suzuki M, Wikarno, Budisantoso, Saefudin I, Itihara M (1985) Fission track ages of pumice tuff. *Quaternary Geology of the Hominid Fossil Bearing Formations in Java*, eds Watanabe N, Kadar D (Geological Research and Development Centre, Bandung, Indonesia), pp 309–357.
26. Swisher, CC, III (1997) A revised geochronology for the Plio-Pleistocene hominid-bearing strata of Sangiran Java, Indonesia. *J Hum Evol* 32:A23.
27. Saleki H (1997) Contribution of nuclear methods intercomparison ($^{230}Th/^{234}U$, ESR and $^{40}Ar/^{39}Ar$) to the dating of Pleistocene fossil bearing layers in the Sangiran dome (Java, Indonesia). PhD thesis (Muséum National d'Histoire Naturelle, Paris) (in French).
28. Hyodo M, et al. (2006) Millennial to submillennial-scale features of the Matuyama-Brunhes geomagnetic polarity transition from Osaka Bay, southwestern Japan. *J Geophys Res* 111:B02103.
29. Schneider DA, Kent DV, Mello GA (1992) A detailed chronology of the Australian impact event, the Brunhes-Matuyama geomagnetic polarity reversal, and global climate change. *Earth Planet Sci Lett* 111:395–405.
30. Kent DV, Schneider DA (1995) Correlation of paleointensity variation records in the Brunhes/Matuyama polarity transition interval. *Earth Planet Sci Lett* 129:135–144.
31. Bassinot FC, et al. (1994) The astronomical theory of climate and the age of the Matuyama-Brunhes reversal. *Earth Planet Sci Lett* 126:91–108.
32. Okada M, Niitsuma N (1989) Detailed paleomagnetic records during the Matuyama-Brunhes geomagnetic reversal, and a direct determination of depth lag for magnetization in marine sediments. *Phys Earth Planet Inter* 56(1-2):133–150.
33. Channell JET, Kleiven HF (2000) Geomagnetic palaeointensities and astrochronological ages for the Matuyama-Brunhes boundary and the boundaries of the Jaramillo subchron: Palaeomagnetic and oxygen isotope records from ODP site 983. *Philos Trans R Soc Lond B Biol Sci* 358:1027–1047.
34. Yamazaki T, Oda H (2001) A Brunhes-Matuyama polarity transition record from anoxic sediments in the South Atlantic (Ocean Drilling Program Hole 1082C). *Earth Planets Space* 53:817–827.
35. Yang T, Hyodo M, Yang ZN, Li HD, Maeda M (2010) Multiple rapid polarity swings during the Matuyama-Brunhes (M-B) transition from two high-resolution loess-paleosol records. *J Geophys Res* 115:B05101.
36. Hyodo M (1984) Possibility of reconstruction of the past geomagnetic field from homogeneous sediments. *J Geomag Geoelectr* 36:45–62.
37. Jin C, Liu Q (2010) Reliability of the natural remanent magnetization recorded in Chinese loess. *J Geophys Res* 115:B04103.
38. Singer BS, et al. (2005) Structural and temporal requirements for geomagnetic field reversal deduced from lava flows. *Nature* 434:633–636.
39. Channell JET, Hodell DA, Singer BS, Xuan C (2010) Reconciling astrochronological and $^{40}Ar/^{39}Ar$ ages for the Matuyama-Burunhes boundary and late Matuyama chron. *Geochem Geophys Geosys* 11:Q0AA12.
40. Koeberl C (1994) Tektite origin by hypervelocity asteroidal or cometary impact: Target rocks, source crators, and mechanisms. *Spec Pap Geol Soc Am* 293:133–151.
41. Glass BP, Pizzuto JE (1994) Geographic variation in Australasian microtektite concentrations; implications concerning the location and size of the source crater. *J Geophys Res* 99:19075–19081.
42. Haines PW, Howard KT, Ali JR, Burrett CF, Bunopas S (2004) Flood deposits penecontemporaneous with ~0.8 Ma tektite fall in NE Thailand: Impact-induced environmental effects? *Earth Planet Sci Lett* 225:19–28.
43. Itihara M, Wikarno, Kagemori Y (1985) Tektites from the Sangiran area. *Quaternary Geology of the Hominid Fossil Bearing Formations in Java*, eds Watanabe N, Kadar D (Geological Research and Development Centre, Bandung, Indonesia), pp 125–133.
44. Aziz F, Shibasaki T, Suminto (1985) Pucung site. *Quaternary Geology of the Hominid Fossil Bearing Formations in Java*, eds Watanabe N, Kadar D (Geological Research and Development Centre, Bandung, Indonesia), pp 87–90.
45. Hartl P, Tauxe L (1996) A precursor to the Matuyama/Brunhes transition-field instability as recorded in pelagic sediments. *Earth Planet Sci Lett* 138:121–135.
46. Shimizu Y, Mubroto B, Siagian H (1985) A paleomagnetic study in the Sangiran area. *Quaternary Geology of the Hominid Fossil Bearing Formations in Java*, eds Watanabe N, Kadar D (Geological Research and Development Centre, Bandung, Indonesia), pp 275–307.
47. Yamei H, et al. (2000) Mid-Pleistocene Acheulean-like stone technology of the Bose basin, South China. *Science* 287:1622–1626.
48. Matsu'ura S, Kondo S, Aziz F, Watanabe N (1995) Chronology of four hominid mandibular fossils newly found from Sangiran and their possible evolutionary implications. *Report of Research Project Supported by Grant-in-Aid from Japanese Ministry of Education, Science, Sports and Culture, Project no. 04454034,* ed and pub Baba H (National Museum of Nature and Science, Tokyo), pp 37–50.
49. Kaifu Y, et al. (2008) Cranial morphology of Javanese *Homo erectus*: New evidence for continuous evolution, specialization, and terminal extinction. *J Hum Evol* 55: 551–580.
50. de Vos J, Sondaar PY, van den Bergh GD, Aziz F (1994) The *Homo* bearing deposits of Java and its ecological context. *Courier ForschungsInstitut Senkenberg* 171:129–140.
51. Matsu'ura S, et al. (2005) Probable source horizon of the *Pithecanthropus* II (Sangiran 2) calotte and its possible palaeoanthropological implications. *Anthropol Sci* 113:323.
52. Jacob T (1966) The sixth skull cap of *Pithecanthropus erectus*. *Am J Phys Anthrop* 25: 243–260.
53. Kondo M, Matsu'ura S, Jacob T (2008) Confirmation of the stratigraphic source of the *Pithecanthropus* VI (Sangiran 10) calotte by the multielement analyses. *Anthropol Sci* 116:253.
54. Aziz F (2007) Faunal stratigraphy of hominid sites in Java, Indonesia: With special reference to vertebrate fossils from Sambungmacan. *Geol Sur Japan Inter Report.* No 42, p 61.
55. Zaim Y, et al. (2011) New 1.5 million-year-old *Homo erectus* maxilla from Sangiran (Central Java, Indonesia). *J Hum Evol* 61:363–376.
56. Danhara T, Yamashita T, Iwano H, Kasuya M (1992) An improved system for measuring refractive index using the thermal immersion method. *Quat Int* 13-14:89–91.
57. Machida H, Arai F (1992) *Atlas of Tephra In and Around Japan* (Univ Tokyo Press, Tokyo).